# Cardiomyocyte behavior on biodegradable polyurethane/gold nanocomposite scaffolds under electrical stimulation

Yasaman Ganji[1,2], Qian Li[2], Elgar Susanne Quabius[3,4], Martina Böttner[5], Christine Selhuber-Unkel[2*], Mehran Kasra[1]

[1] *Faculty of Biomedical Engineering, Amirkabir University of Technology, 424 Hafez Ave, Tehran, Iran*

[2]*Institute for Materials Science, Dept. Biocompatible Nanomaterials, University of Kiel, Kaiserstr. 2, D-24143 Kiel, Germany*

[3]*Dept. of Otorhinolaryngology, Head and Neck Surgery, University of Kiel, Arnold-Heller-Str. 3, Building 27, D-24105 Kiel, Germany*

[4]*Institute of Immunology, University of Kiel, Arnold-Heller-Str. 3, Building 17, D-24105 Kiel, Germany*

[5]*Department of Anatomy, University of Kiel, Kiel, Germany*

*Corresponding author:

Christine Selhuber-Unkel; University of Kiel, Institute for Materials Science, Kaiserstr. 2, 24143 Kiel, Germany

Tel.: +49 431 880 6198

Fax: +49 431 880 6290

Email address: cse@tf.uni-kiel.de

**Abstract**

Following a myocardial infarction (MI), cardiomyocytes are replaced by scar tissue, which decreases ventricular contractile function. Tissue engineering is a promising approach to regenerate such damaged cardiomyocyte tissue. Engineered cardiac patches can be fabricated by seeding a high density of cardiac cells onto a synthetic or natural porous polymer. In this study, nanocomposite scaffolds made of gold nanotubes/nanowires incorporated into biodegradable castor oil-based polyurethane were employed to make micro-porous scaffolds. H9C2 cardiomyocyte cells were cultured on the scaffolds for one day, and electrical stimulation was applied to improve cell communication and interaction in neighboring pores. Cells on scaffolds were examined by fluorescence microscopy and scanning electron microscopy, revealing that the combination of scaffold design and electrical stimulation significantly increased cell confluency of H9C2 cells on the scaffolds. Furthermore, we showed that the gene expression levels of Nkx2.5, atrial natriuretic peptide (ANF) and natriuretic peptide precursor B (NPPB), which are functional genes of the myocardium, were up-regulated by the incorporation of gold nanotubes/nanowires into the polyurethane scaffolds, in particular after electrical stimulation.

*Keywords: Adhesion, Cardiac tissue engineering, Gold nanotube/nanowire, Nanocomposite, Biodegradable polyurethane, electrical stimulation*

## 1. Introduction

Cardiovascular diseases pose the highest risk of death in the world, according to the American Heart Association Statistics. Every 34 seconds one American dies by heart attack, stroke or other cardiovascular problems [1]. Currently, treatment options following a myocardial infarction (MI) and subsequent congestive heart failure are still limited. Pharmacological agents increase the blood flow but limit ventricular remodeling events and increase cardiac output [2]. Mechanical devices, such as the left ventricular assist device (LVAD), can only be applied to a limited group of patients [3]. The only successful treatment option for a severe MI to date is heart transplantation [4]; however, the lack of suitable donors significantly restricts this option.

As cardiovascular diseases remain a major cause of morbidity and mortality, new strategies in cardiovascular treatments attract much attention. Among all cardiovascular diseases, MI is one of the key reasons for heart failure, resulting in heart dysfunction and progressive death of cardiomyocytes when normal heart function cannot be restored afterwards [5]. Cell therapy has so far shown only little improvement of cell retention and long-term survival [6]. Instead, biocompatible 3D scaffold materials might provide a feasible solution, as some structures may improve cell retention, survival and even cell differentiation [7, 8]. These kinds of scaffolds or patches can, in principle, be directly implanted on the infarcted tissue with or without cells after MI [9].

Typically, tissue engineering for cardiovascular regeneration is based on producing biomimetic and biodegradable materials for scaffold fabrication [4] that ideally integrate signaling molecules and induce cell migration into the scaffolds [10, 11].

A material suitable for a tissue engineering-based approach to treat myocardial infarction should provide an environment that is predisposed to improve electromechanical coupling of the

cardiomyocytes with the host tissue [10, 12], as well as cardiomyocyte adhesion [9]. This adhesion is essential for the proliferation of cardiomyocytes and for ventricular function. Materials suitable for application in cardiac tissue engineering include natural polymers, such as decellularized myocardium [13], collagen [14], alginate [15], fibrin [16], as well as synthetic polymers such as polylactic acid (PLA), polyglycolic acid (PGA), their copolymers [17, 18], and polyurethane (PU) [19, 20].

Among the above-mentioned materials, PUs are considered a major class of applicable elastomers because of their good biocompatibility and biodegradability, their high flexibility, and their excellent mechanical properties [21, 22]. The stiffness of heart muscle varies from 10 kPa in the beginning of the diastole to 500 kPa at the end of the diastole, therefore an elastic material having a stiffness in this range would be required for cardiac engineering [23]. Such Young's moduli are obtained with biodegradable PUs [19, 24], which can be synthesized by using vegetable oils as polyol and aliphatic diisocyanate, resulting in typical degradation times of several months. Among different grades of PUs, castor oil-based PU shows no toxicity, is low in cost, and is available as a renewable agricultural resource [25-27]. This grade of biodegradable PUs has already been widely applied in biomedical engineering, including materials for peripheral nerve regeneration, cardiovascular implants, cartilage and meniscus regeneration substrates, cancellous bone substitutes, drug delivery carriers and skin regeneration sheets [28-30].

Furthermore, tissue engineering applications require that cells are embedded into the material. Much progress has recently been made in order to fabricate porous polymer scaffolds, in particular by using salt leaching techniques [31-33]. The success of this method has been shown

for a variety of soft and hard polymers [34-37], and we have recently established this procedure for PU [38].

Although many PU-based materials have been developed for providing vascular grafts, only few PU scaffolds have so far been studied in the context of myocardial tissue engineering [39, 40], even though PU is easy to implant into muscle tissue, because it is stiffer than typical hydrogels. An important goal for myocardial tissue engineering must be the fabrication of materials that allow for the synchronization of electrical signals, and thus enhance the contraction of cardiomyocytes in the scaffold material so that a homogeneous total contraction of the engineered patch is guaranteed. In the study presented here, we fabricated a biodegradable nanocomposite material by incorporating gold nanotubes/nanowires into PU scaffolds so that the wired material structure can mimic the electromechanical properties of the myocardium.

To investigate the functionality of these materials as cardiac patches, H9C2 rat cardiomyocyte cells were seeded on different polyurethane-gold nanotube/nanowire (PU-GNT/NW) composites. Eventually, electrical stimulation was applied to the cell-scaffold constructs in order to enhance the functional performance of cardiac scaffolds and to improve cell morphology and alignment. We used fluorescence and scanning electron microscopy as well as gene expression analysis to investigate the behavior of cardiomyocyte cells on the scaffolds. We demonstrate that the adhesion and proliferation of cells significantly depends on the amount of incorporated GNT/NW, and that an optimum concentration of 50 ppm of GNT/NW can provide the best environment for cells to achieve native cardiomyocyte function.

## 2. Materials and methods

### 2.1. Synthesis of polyurethane-GNT/NW composite scaffolds

Polyurethane-GNT/NW composites were synthesized according to our previous work [38]. In brief, gold nanotubes/nanowires (GNT/NW) were made by using template-assisted electrodeposition and mixed with castor oil /polyethylene glycol-based polyurethane (PU). Concentrations of 50 and 100 ppm of GNT/NW were used to synthesize two different composites types. For fabrication of porous scaffolds, 355-600 μm sieved table salt was added to the PU-GNT/NW solution, then the mixture of PU-GNT/NW and salt was cast in a Teflon mold of 10 mm diameter and 4 mm thickness. Afterwards, all samples were dried at room temperature for 48 hours; then the porous scaffolds were placed in distilled deionized water (DDW) for 2 more days to remove the salt. In the following, we refer to the scaffolds as PU-0 for pure PU scaffolds, PU-50 for scaffolds containing 50 ppm GNT/NW, and PU-100 for those containing 100 ppm GNT/NW.

### 2.2. Permeability

As it is experimentally difficult to obtain 3D information about pore interconnectivity based on 2D images, Li et al. [41] suggested a simple method of soaking the samples in an ink solution and then imaging the colored sample. Accordingly, our scaffolds were soaked in a solution of common blue writing ink for 24 hours and dried at room temperature. Then, a cross section of samples with a thickness of 1 mm was prepared by cutting with a surgical blade and then imaging the samples with a Nikon (TS100) inverted microscope (10X objective). This treatment provides information on the interconnectivity of pores as well as on their accessibility from

neighboring pores. Porosity was calculated by ImageJ [42] using a manually set intensity threshold.

### 2.3. Cell culture and electrical stimulation

H9C2 rat cardiomyocytes were purchased from the European Collection of Cell Cultures (ECACC, Germany) and maintained in Dulbecco's Modified Eagle's medium (DMEM, Biochrom, Germany), supplemented with 10% fetal bovine serum (FBS, Biochrom, Germany) and 1% penicillin and streptomycin (100 U/ml, Biochrom, Germany) at 37 ºC and 90% humidity. H9C2 is a subclone of the original clonal cell line derived from embryonic rat heart tissue. Cells were sub-cultured regularly and used up to passage 6. Prior to the experiments, PU scaffolds were sterilized using ethylene oxide gas and placed in 10 ml of sterilized phosphate buffered saline (PBS) for 2 hours. Cells ($10^6$) were seeded per cylindrical scaffold (diameter: 10 mm, thickness: 4 mm) and incubated overnight to allow cell attachment. On the following day, cells were stimulated using a function generator (Toellner, Germany) with a square pulse of 1 V/mm amplitude, pulse duration of 2 ms, at a frequency of 1 Hz for 15 minutes. This procedure was repeated on three consecutive days, once per day [43, 44]. Stainless steel 304 was used as the electrode material for electrical stimulation. Compared to titanium electrodes and titanium electrodes coated with titanium nitrate, the electrical field was stable in stainless steel 304 electrodes over the whole time of stimulation [43]. The cell-scaffold constructs were left in the incubator for one more day.

### 2.4. Staining with Calcein and Hoechst

Calcein was used for staining viable cells and Hoechst for staining cell nuclei. Five repeats of each scaffold group were stained with both Calcein AM and Hoechst after 1 day of cell culture before stimulation and another 5 repeats of each group were stained on the fourth day after cell seeding and electrical stimulation. For Calcein staining, the samples were rinsed once with DMEM and incubated with a 1 µg/ml solution of Calcein (BD Bioscience, Germany) in DMEM for 10 minutes at 37ºC. Afterwards, the samples were washed with DMEM twice, stained with 10 µg/ml Hoechst 32258 (Invitrogen, Germany) in PBS and incubated for 20 minutes at 37 ºC. Then, the samples were washed extensively with PBS and imaged using an Olympus BX43 fluorescence microscope (Olympus, Japan) with a 10X objective. Cell confluency was measured as the ratio of the area stained with Calcein to the whole surface of a scaffold in 2D images using ImageJ [42]. This test was performed in two independent experiments and at least 5 images were taken in each experiment.

### 2.5. Gene expression

Cells were lysed in TriSure (Bioline, Luckenwalde, Germany) and RNA extraction was performed according to the manufacturer's protocol. In order to obtain enough RNA, cells grown on 3 scaffolds were pooled. After RNA extraction, aliquots of 200 ng total RNA from each group were reverse transcribed into cDNA, using a cDNA synthesis kit (AmpTec, Hamburg, Germany) and the provided oligo dT-V primer. Subsequently the cDNAs were purified utilizing the spin columns and buffers provided with the cDNA synthesis kit. Gene expression was analyzed by qRT-PCR using a Rotorgene 3000 (Corbett, LTF, Wasserburg, Germany). For each qRT-PCR analysis, 2.5 µl of the above-mentioned cDNA (=10 ng total RNA) was used; total reaction

volume was 25 µl each and cycling conditions were as follows: 10 min initial denaturation at 95°C followed by 45 cycles of 20 s denaturation at 95°C, 20 s annealing, for details see table 1, and 20 s elongation at 72°C. At the end of the cycling program a melt curve analysis was performed starting at the actual annealing temperature. All samples were run in duplicates. Gene-specific primers were obtained from TibMolBiol (Berlin, Germany). Primers for atrial naturiuretic factor (ANF), Connexin 43 (Con43), Cardiac troponin I (cTnl; Tro I), cardiac Troponin T type 2 (Tnnt2; Tro II), NK2 homeobox 5 (Nkx2.5), Myocyte enhancer factor 2C (Mef2c) and glyceraldehyde-3-phosphate dehydrogenase (GAPDH) were designed using the web-based "Primer 3" program. Primers for ß-cardiac myosin heavy chain (β-MHC), natriuretic peptide B (NPPB) and GATA binding protein 4 (GATA 4) were published previously [45, 46]; as were the primers for Beta-2-microtubulin (B2M), TATA box binding protein (TBP) [47] and those for 18S ribosomal protein mRNA (18sr RNA) [48]. The SYBR Green based qPCR mix was purchased from Peqlab (Erlangen, Germany). Threshold levels for Ct-determination were chosen manually. Primer sequences and annealing temperatures are provided in table 1.

### 2.6. Scanning Electron Microscopy

The morphology of the porous Polyurethane-GNT/NW nanocomposites was studied by field emission scanning electron microscopy (FESEM; Philips S-4160).

For observation of cell-scaffold constructs, the samples were fixed in 3% glutaraldehyde (Sigma-Aldrich, Germany) solution in PBS, and then dehydrated with a graded ethanol (Walter CMP, Germany) series (30%, 50%, 70%, 80%, 90%, 96%), 20 minutes each. Dehydration was finished with 100% ethanol overnight. The samples were sectioned with the thickness of 7 µm from the top side, further dehydrated using a critical point dryer (CPD 030, Balzers, Switzerland), and

198 coated with gold (Ion Tech Ltd., Teddington, U.K.) before SEM imaging (XL 20, Philips, The
199 Netherlands).

200 **Table 1.** Primer sequences and annealing temperatures for qRT-PCR analysis of the
201 housekeeping and target genes.

| Gene symbol and accession number | Gene name | Primer sequence [5'--3'] | Annealing temperature [°C] |
|---|---|---|---|
| ANF<br>NM_012612.2 | Atrial Naturiuretic factor | forward: atcaccaagggcttcttcct<br>reverse: ccaggtggtctagcaggttc | 64 |
| GAPDH<br>NM 017008 | Glyceraldehyde-3-phos-phate dehydrogenase | forward: ggcattgctctcaatgacaa<br>reverse: tgtgagggagatgctcagtg | 60 |
| β-MHC<br>X15939.1 | ß-cardiac myosin heavy chain | forward: gagtggacgtttattgacttcgg<br>reverse: gcctttctttgctttgccttt | 64 |
| NPPB<br>NM_031545 | Natriuretic peptide B | forward: cagctctcaaaggaccaagg<br>reverse: cggtctatcttctgcccaaa | 64 |
| GATA4<br>NM_144730.1 | GATA binding protein 4 | forward: gtgccaactgccagactacc<br>reverse: agccttgtggggagagcttc | 62 |
| B2M<br>NM_012512.2 | Beta-2-microtubulin | forward: ccgtgatctttctggtgctt<br>reverse: atttgaggtgggtggaactg | 60 |
| TBP<br>NM_001004198.1 | TATA box binding protein | forward: ttctgggaaaatggtgtgc<br>reverse: cccaccatgttctggatctt | 60 |
| 18sr RNA<br>NM_078617.3 | 18S ribosomal protein mRNA | forward: accgcggttctattttgttg<br>reverse: ctgatcgtcttcgaacctcc | 60 |
| Con43<br>AH003191.2 | Connexin 43 | forward: tgaaagagaggtgcccagaca<br>reverse: cgtgagagatggggaaggact | 60 |
| cTnl (Tro I)<br>M57679.1 | Cardiac troponin I | forward: gccctcaaacttttttctttcgg<br>reverse: ctgatgctgcagattgcgaag | 60 |
| Tnnt2 (Tro II)<br>NM_012676.1 | Troponin T type 2 (cardiac) | forward: caaggaacagagctttgtcgaa<br>reverse: cacaacctagaggccgagaagt | 60 |
| Nkx2.5<br>NM_053651.1 | NK2 homeobox 5 | forward: cgcccttctcagtcaaagac<br>reverse: gaaagcaggagagcacttgg | 62 |
| Mef2c<br>XM_006231731.2 | Myocyte enhancer factor 2C | forward: ttgccttccctgttcatacc<br>reverse: ggcaaaccatctgaagcaat | 60 |

202 **2.7. Statistical analysis**

203 Cell confluency is presented as mean value ± standard deviation. Differences between groups
204 were analyzed by analysis of variance (ANOVA) followed by Tukey's multiple comparison test.

For gene expression analysis, the results are presented as mean value ± standard deviation. qRT-PCR data were analyzed according to the ΔΔCt method [30] using the mean Ct value of the housekeeping genes. Fold changes of expression levels were calculated as described previously [30] and the obtained values were used for statistical analysis.

## 3. Results

### 3.1. Permeability of the scaffolds

An essential prerequisite for a cardiac patch material is to ensure porosity above the percolation threshold, so that the cells can grow deeply into the scaffold without undergoing hypoxia-induced cell death. In figure 1, we present images of scaffold cross-sections after incubation in ink. Our results show that all imaged scaffolds were homogeneously colored by the ink, regardless of their GNT/NW content. This confirmed that the pores were almost uniformly distributed and interconnected. Colored pores were found to be accessible either directly or via adjacent pores. The porosities of the scaffolds were above 90% in all samples. By increasing the amount of gold content in the polymer solution during polymerization, the interconnectivity of the pores was improved, presumably due to the presence of chloroform in the gold-containing samples, which leads to the activation of a solvent casting mechanism in addition to salt leaching. Furthermore, we observed that PU-100, having the highest gold content and smallest polymer concentration, was the most uniform in pore size and distribution and had the largest pores (Fig. 1 c). SEM images of scaffolds also confirmed the largest pores in PU-100 (Fig. 1 d) compared to PU-0 or PU-50 (Fig. 1 e-f)

### 3.2. Cell adhesion and growth on scaffolds

Cells of the myocardium need to adhere and proliferate on the material patch in order to form a functional cell network before the scaffold material is degraded. To compare how cell adhesion and growth are influenced by the different scaffold types and by additional electrical stimulation, we investigated the morphology of H9C2 cells stained with Calcein (cell body) and Hoechst (nucleus) on different scaffolds with and without electrical stimulation in figure 2. Figures 2a-c clearly show that cells after 1 day of incubation spread best on PU-50 compared to PU-0 or PU-100, and they are more homogeneously distributed within the scaffolds than cells on the other two scaffold types (PU-0 and PU-100). In particular, on the PU-100 scaffold H9C2 cells preferred to attach to each other and formed large clumps rather than spreading on the sample. On samples that had undergone electrical stimulation, the results were distinctly different: whereas cell spreading was not significantly influenced by electrical stimulation on PU-0 scaffolds, it was significantly enhanced on the gold-containing PU-50 and PU-100 scaffolds. This observation is even more pronounced in the quantitative analysis of confluency (Figure 3).

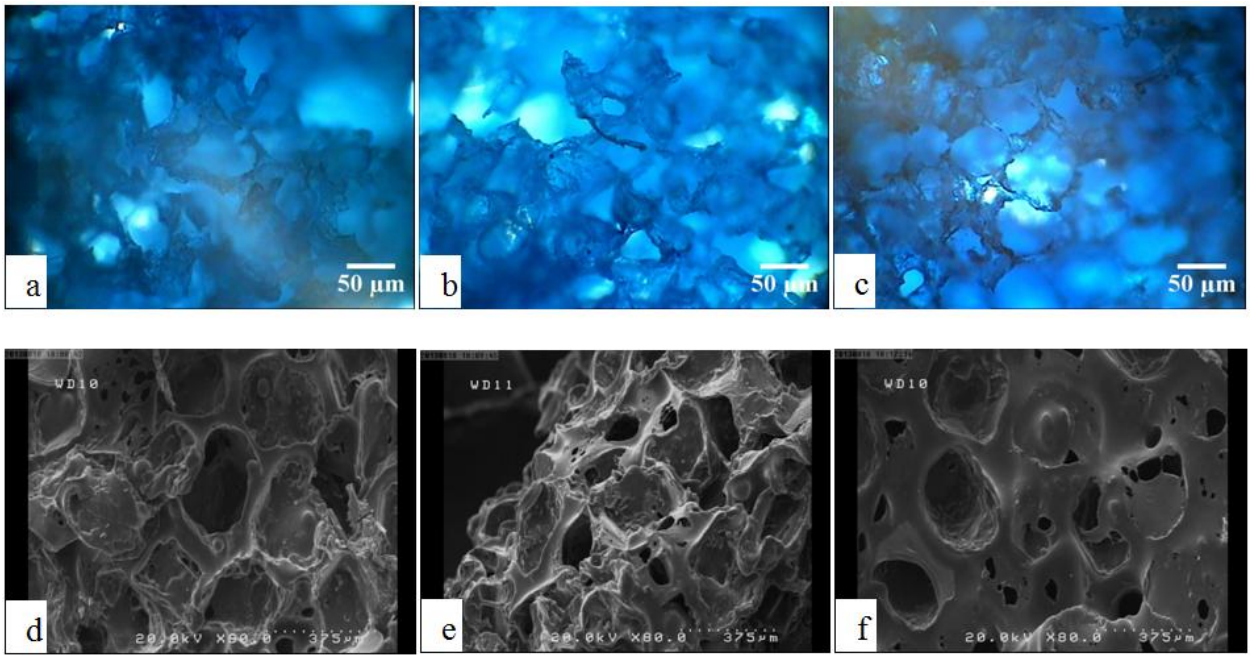


**Fig. 1.** (a)-(c) Light microscopy image demonstrating the permeability of ink into the pores. (a) PU-0, (b) PU-50, and (c) PU-100. The pores are interconnected and almost uniform in size throughout the cross-section of the scaffold materials. SEM images show the structure of pores in different samples of (d) PU-0, (e) PU-50, and (f) PU-100. PU-100 showed the most interconnected and the largest pores compared to PU-0 or PU-50.

Furthermore, we checked if cell alignment after electrical stimulation was enhanced which would mimic the natural response of cells to electromechanical coupling in the heart. The representative images in Fig. 2 clearly show that the cells were aligned only in gold-containing scaffolds, whereas no alignment was observed in PU-0. Furthermore, no significant differences in cell alignment were observed when cells were seeded on PU-50 and PU-100 scaffolds.

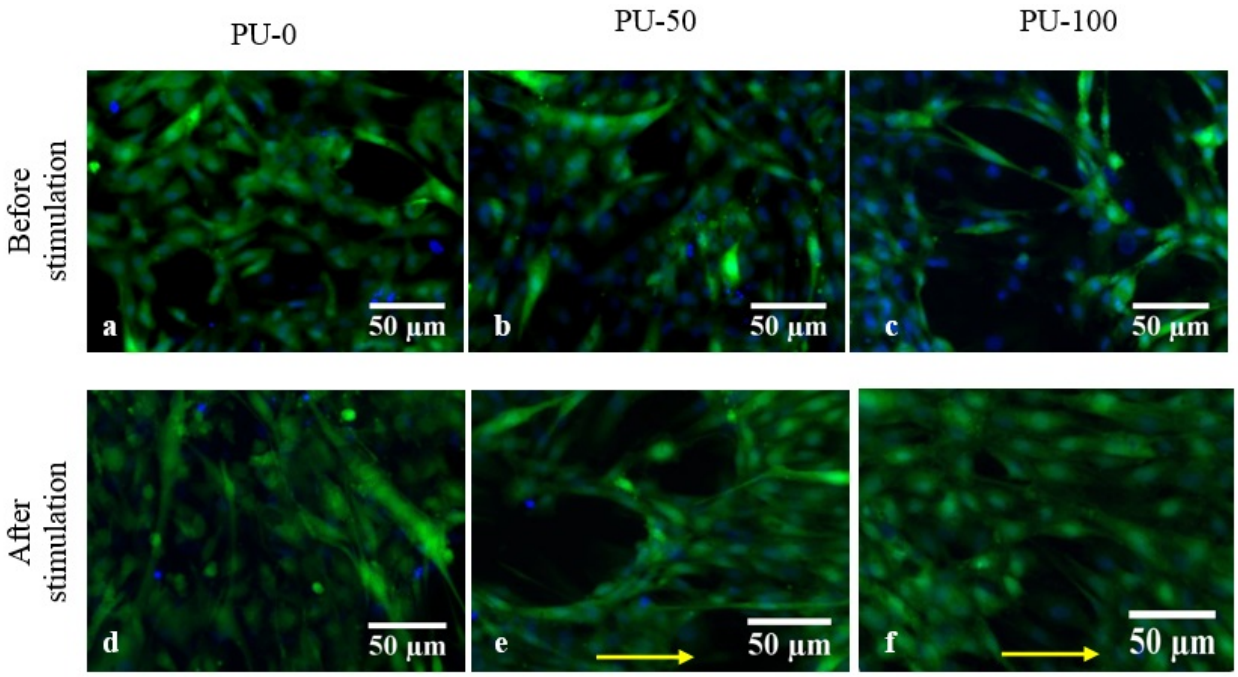


**Fig. 2.** Staining of H9C2 cells nuclei (Hoechst, blue) and cytoplasm (Calcein, green) before (a, b, c; cells cultured 1 day) and after (d, e, f; cells cultured 4 days) electrical stimulation on PU-0 (a, d), PU-50 (b, e) and PU-100 (c, f). Scale bar is 50 µm. Arrows indicate the direction of cell alignment.

Figure 3 summarizes our results for H9C2 cell confluency on scaffolds before and after stimulation. Confluency increased by 39% and 14% after stimulation for PU-50 and PU-100 scaffolds, respectively. However, at the same time cell confluency was not significantly influenced by electrical stimulation in the samples without gold (PU-0). When the samples were incorporated with gold, a significant increase was found between PU-0 and PU-50 after stimulation. An even more marked increase was found for PU-50 before and after stimulation, however for PU-100, no significant difference was found.

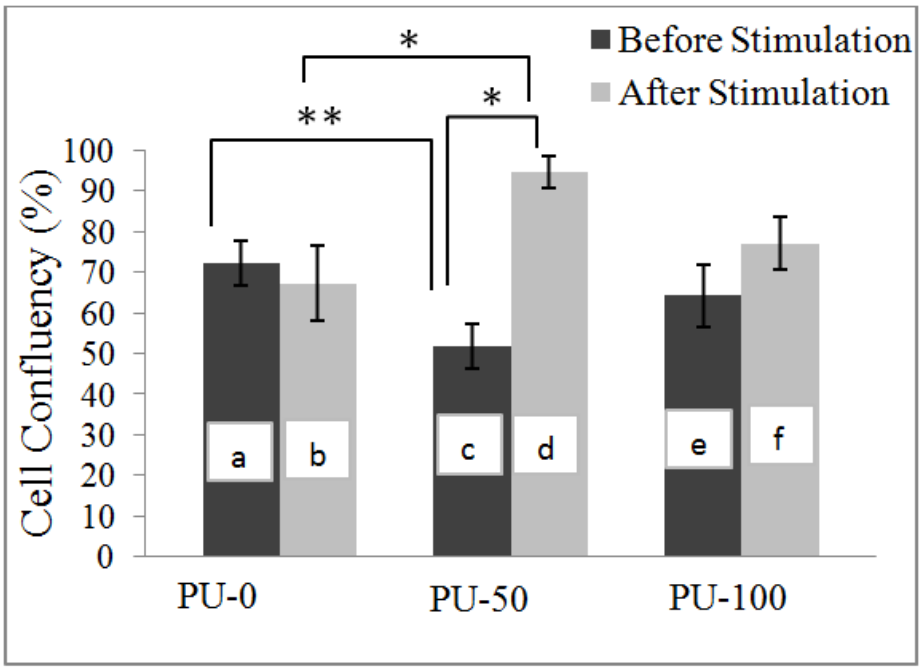


**Fig. 3.** Cell confluency on scaffolds before (a, c, e) and after (b, d, f) electrical stimulation. ANOVA analysis was used for evaluating data significance (*$p < 0.05$, **$p < 0.01$).

### 3.3. Gene expression

In order to investigate if the incorporation of gold into porous PU scaffolds in combination with electrical stimulation can facilitate the function of H9C2 cardiomyocyte on the scaffolds similarly to native myocardium, we investigated the expression of several relevant genes using qRT-PCR analysis. To this end, we evaluated gene expression levels of different cardiac transcription factors (GATA4, NPPB, ANF, and β-MHC) as well as gene expression levels of Con43, cTnl (Tro I), Tnnt2 (Tro II), Nkx2.5 and Mef2c in the H9C2 cardiomyocytes on different scaffolds and as a function of electrical stimulation. The expression levels of the housekeeping genes GAPDH, B2M, TBP and 18sr RNA were also examined. Expression levels of GAPDH, B2M, TBP and 18sr RNA were not significantly affected by any of the treatments (fold changes

<2; data not shown) and were therefore used to normalize gene expression levels of the genes of interest, namely GATA4, NPPB, ANF, β-MHC, Con43, cTnl (Tro I), Tnnt2 (Tro II), Nkx2.5 and Mef2c.

Figure 4 shows ANF, NPPB, Tnnt2 (Tro II), Nkx2.5 and Mef2c gene expression in H9C2 cardiomyocytes. In Fig. 4a and c, Δct values obtained in cells grown on normal culture dishes (as control group) were set as "1" and fold changes obtained in cells grown on PU-0, PU-50, PU-100 were calculated as described elsewhere [30]. Similarly in Fig. 4b and d, values obtained from cells grown on pure PU-0 scaffolds alone were set as "1" and fold changes obtained in cells grown on PU-50 or PU-100 were calculated as described elsewhere [30]. Dotted lines indicate 2-fold changes of gene expression as described previously and ± 2-fold changes in gene expression levels are considered statistically significant [30].

Compared to tissue culture plastic surfaces, all our PU samples showed, regardless of their GNT/NW content, upregulated gene expression of some cardiac transcription factors in H9C2 cells. ANF, NPPB, Tnnt2 (Tro II), Nkx2.5 and Mef2c expression levels were already increased when H9C2 cells were grown on pure PU-0 scaffolds (3.26±0.22 fold (ANF), 111.3±4.82 fold (NPPB), 3.27±0.22 (Mef2c), 27.76±2.29 (Nkx2.5) and 6.49±1.29 [Tnnt2 (Tro II)]) compared to cells grown in normal culture dishes. Growing the cells on PU-50 resulted in a distinct increase of ANF, NPPB and Nkx2.5 expression levels, which were 15.6±0.73, 560.76±3.58 and 79.34±1.76 times higher, respectively, than those detected in cells grown in normal culture dishes. Gene expression levels of Mef2c and Tnnt2 were only marginally increased when cells were grown on PU-50 (3.31±0.22 for Mef2c and 7.82±0.16 for Tnnt2). Expression changes of the cells growing on PU-100 were as follows: 8.2±0.49 fold increase of ANF- and 240.1±5.44 fold increase of NPPB-expression, when compared to the levels detected in cells grown in

298 normal culture dishes (Fig. 4a); Mef2c gene expression was only 1.62±0.11 times higher when
299 cells were grown on PU-100, similarly Nkx2.5 was only 31.94±1.19 times higher when
300 compared to cells grown in normal culture dishes and Tnnt2 gene expression levels were
301 10.41±1.16 higher (Fig. 4c). Interestingly, the fold changes in ANF- and NPPB-expression, when
302 compared to levels detected in cells grown on PU-0 were rather similar: 4.78±0.23 and
303 4.94±0.31 in ANF- and NPPB-expression, respectively, in cells grown on PU-50 and 2.52±0.11
304 and 2.12±0.09ANF- and NPPB-expression, respectively, in cells grown on PU-100 (Fig. 4b).
305 This, however, was not the case for Mef2c, Nkx2.5 and Tnnt2 leading for Mef2c gene expression
306 a 2.01±0.26 fold decrease when grown on PU-100 and a 2.86±0.26 fold increase when grown on
307 PU-50, while all other conditions were not significantly influenced, and Tnnt2 expression was
308 not at all affected when compared to PU-0 scaffolds (Fig. 4d). GATA 4, Con43 and cTnl (Tro I)
309 expression was not affected by any of the different scaffolds, and β-MHC expression could not
310 be detected in these cells, but was detectable in cDNA synthesized from total RNA of normal rat
311 embryonic tissue (Rat RNA: 17-19 days; amsbio biotechnology, Abingdon, United Kingdom),
312 which was used as a positive amplification control (data not shown).

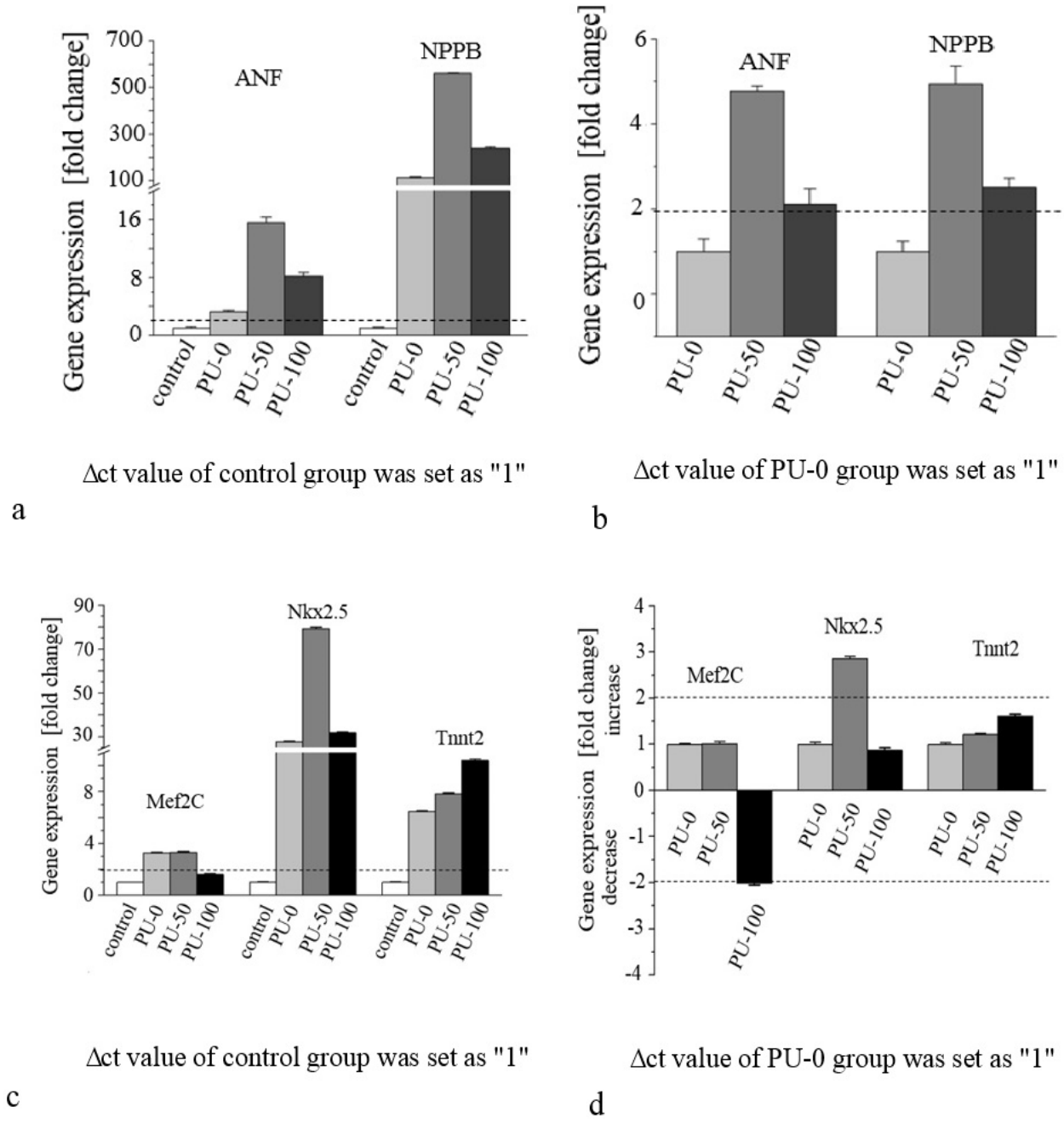


313

314 **Fig. 4.** Fold change in (a, b) ANF, NPPB; and (c, d) Mef2C, Nkx2.5 and Tnnt2 gene expression
315 in H9C2 cardiomyocytes. Δct values obtained in cells grown on (a, c) normal culture dishes
316 (control) and (b, d) on pure PU, were set as "1". Dotted lines indicate a 2-fold change of gene

317 expression and gene expression changes above such a 2-fold change were considered statistically
318 significant.

319 ### 3.4. Scanning Electron Microscopy

320 SEM images of H9C2 cells on different samples after 3 days of electrical stimulation are shown
321 in figure 5. The images clearly support our findings from the cell staining experiments, as more
322 cells are adhering to the PU-50 scaffold than to the other scaffolds. Furthermore, cells adhering
323 to PU-100 had a morphology similar to cardiomyocytes in native tissue. The results are in
324 agreement with our results on cell confluency, as there are more cells adhering to PU-50 than to
325 the other scaffolds. In general, imaging cells inside porous scaffolds was very challenging due to
326 the spatial conformation of pores, in which the cells can hide behind the pore walls (Fig. 5d).
327 These results prove that our nanocomposite scaffolds indeed support cell attachment much better
328 compared to gold-free PU-0 scaffolds. This is probably due to a larger number of interconnected
329 pores in the gold-containing samples, providing higher probabilities for cells to grow through the
330 scaffold pores, thus improving cell adhesion and proliferation.

331 ## 4. Discussion

332 In the work presented here, we investigated a novel method using the combined effect of a
333 polyurethane-gold nanotube/nanowire composite material and electrical stimulation of
334 cardiomyocyte cells. This specific composite material of nano-sized gold incorporated into a
335 porous biodegradable polyurethane matrix was chosen in order to improve the transmission and
336 synchronization of electrical signals in the material and thus increase the natural functionality of
337 cardiomyocytes. The feasibility of this approach of incorporating gold nanoparticles into scaffold

materials for applications such as cardiac patches has recently been shown for an alginate matrix [49]. Such alginate matrices have a very low elastic modulus of only a few kPa and are viscoelastic [50].

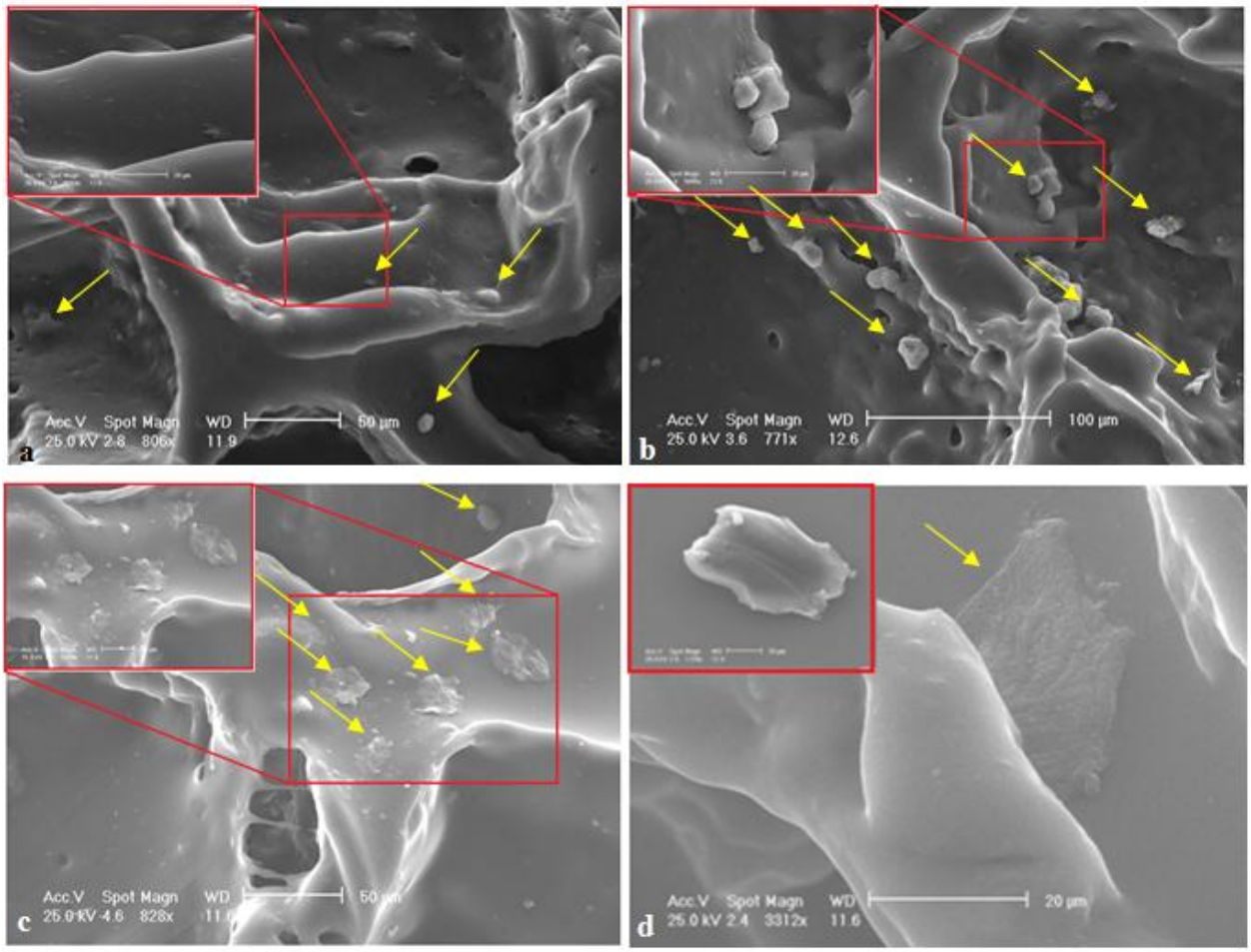


**Fig. 5.** SEM images of cells on (a) PU-0, (b) PU-50, and (c) PU-100 on day 4 after electrical stimulation. (d) A single cell cultured on PU-100 hiding behind the pore walls, a single cardiomyocyte cell cultured on glass slide is shown in the inset. Cells spread better on those samples containing gold and the best cell spreading is obtained on PU-100. Arrows point at single cells.

An ideal material for cardiac tissue engineering would, however, be purely elastic in order to mimic the complicated mechanical properties of native heart tissue without tearing during systolic pressure or prohibiting contractile force. The compressive modulus of native heart tissue has been reported to be 425 kPa at the systole [49]. We have recently shown that PU-GNT/NW composites can provide the mechanical properties required for this purpose, i.e. elasticity can be tuned between 200 kPa and 240 kPa [38]. Incorporation of gold nanoparticles in PU substrates changed the physicochemical properties of PU and improved fibroblast cell attachment [51], and gold in the form of nanowires allowed the formation of conductive bridges between pores and enhanced cell communication [38, 49]. Addition of GNT/NW caused the formation of hydrogen bonding with the polyurethane matrix and improved the thermomechanical properties of nanocomposites. Higher crosslink density and better cell attachment and proliferation were reported in polyurethane containing 50 ppm GNT/NW [38]. Additionally, PU and PU composites showed controllable degradation properties using different polyols during the synthesis process [21, 22]. The polymeric matrix in PU-GNT/NW composites can therefore be replaced by extracellular matrix (ECM) due to the controlled degradation of PU [52, 53]. After degradation of the scaffold matrix, the gold nanoparticles would remain in the cardiac muscle ECM, which should not harm the cardiac tissue as the gold concentration is comparably low, thus cytotoxicity should be negligible [54]. Additionally, the concentration of gold in most 3D structures varies from 0.0001 % wt. to 15 % wt. and the low concentration of ppm has been shown to affect the cellular activity [55].

Since intact myocardium tissue contains a high density of cardiomyocytes and is known for heavy oxygen consumption, pore interconnectivity and pore uniformity are essential properties of any tissue engineered cardiac patch material, as they guarantee nutrition and oxygen

exchange. Both are, for example, necessary to facilitate cell migration [56]. Additionally, the size and orientation of pores has been reported to affect cell alignment [57]. We used 355-600 μm sieved table salt in scaffold fabrication by a porogen-leaching method so that a microscopic, interconnected, and homogeneous pore structure was formed (Fig. 1). Nutrients should therefore easily be transported deeply into the scaffolds.

In addition to the relevance of material selection for cardiac tissue engineering, signaling factors also play a major role for engineering a functional tissue patch. Proper signaling might be induced by mechanical stimulation or electrical stimulation, similar to the conditions found in intact myocardium. A recent study has shown that in heart mimicking constructs, applying only mechanical stimulation was not a proper signaling factor to keep cardiomyocytes functional [58]. Instead, it has been suggested that an excitation-contraction coupling in cell-scaffold constructs is required for the proper function of cardiomyocyte tissue. This can be achieved by electrical stimulation just as in native heart, where the mechanical stretch of the myocardium is induced by electrical signals [58]. Other studies have already shown that even small physiological fields (75-100 mV/mm) can stimulate the orientation, elongation and also migration of endothelial cells [12].

In this study, we investigated the orientation and adhesion of cardiomyocyte cells on different PU scaffolds after 3 days of consecutive electrical stimulation (Fig. 2). Only on gold-containing scaffolds cells had changed their alignment after four days. Before stimulation, no significant difference of cell morphology was found, whether gold had been incorporated in the scaffolds or not. Furthermore, cell proliferation was not enhanced as a result of gold incorporation. On PU-0, no cell alignment was observed even after electrical stimulation; on both PU-50 and PU-100, cells were aligned on day 4 after electrical stimulation. It is interesting that after stimulation, PU-

50, not PU-100, showed the greatest amount of cells, although cells showed on PU-100 a morphology that was most similar to their natural morphology.

In our experiments, the alignment of cells was rearranged towards the direction of the applied electrical field. A similar cell alignment improvement was reported by Au et al. [59] for fibroblasts and cardiomyocytes. Furthermore, the cells were re-oriented due to electrical stimulation only on PU-GNT/NW composites (Fig. 2). Particularly for endothelial cells, it is well-known that electrical stimulation can change cell elongation, alignment, and migration [10]. Here, we made use of this effect in order to electrically polarize the cardiomyocytes seeded on PU-GNT/NW scaffolds to provide a better microenvironment for their adhesion, elongation and function.

It has previously been reported that a square, biphasic electrical pulse of 2 ms duration provided cell coupling similar to that present in *in vivo* environments after 8 days of stimulation [58] and a small electrical field of 200 mV/mm caused a fully-oriented cell network [12]. Despite all of these electrical stimulations, Tandon et al. [44] showed that the alignment of cardiomyocyte cells was only affected by surface topography and not by applying an electrical field; however, our result demonstrated that electrical stimulation indeed facilitates the behavior of only those cell-scaffold constructs that contained gold.

The morphology and distribution of cells investigated by SEM confirmed the essential role of pore size and distribution in the scaffolds (Fig. 5). We observed a marked difference in terms of both cell number and cell morphology between pure PU and PU-GNT/NW composites. In PU-GNT/NW composites, where chloroform had been used during fabrication, the pores were bigger and more interconnected (Fig. 1). Therefore, more cells could migrate into the scaffold and could easily be observed. However, we found that cells on PU-100 were closer to their native

morphology. This is consistent with our previous result that 50 ppm gold provides optimum adhesion conditions for mesenchymal cell attachment [38], presumably by changes in surface energy in response to the incorporation of gold. Other studies have shown that an optimum amount of gold (43-50 ppm) caused a microphase separation in the chemical composition of PU, hence improving hydrophilicity [55]. Gold nanoparticles in a concentration of 43.5 ppm in polyurethane matrix have been shown to cause minimum inflammatory response *in vitro* and *in vivo*, and improve biocompatibility [51]. Our study shown here suggests that the PU-50 scaffolds provide optimum conditions for a cardiac tissue engineering material.

Our gene expression analysis of specific markers in myocardium tissue clearly showed changes in the expression levels of functional cardiac genes, clarifying the role of gold nanoparticle incorporation into PU and the importance of electrical stimulation. Five different specific genes were investigated (Fig. 4). The expression of both ANF and NPPB was significantly up-regulated (Fig. 4a); the highest up-regulation level was determined on PU-50. The ANF gene is highly expressed by cardiomyocytes when arteriosclerosis has occurred and a decrease has been reported during maturation of ventricular cells [40]. ANF is particularly a marker of cardiomyocyte differentiation [60, 61]. Therefore, the marked increase of this gene's expression in PU-50 and PU-100 found here is assumed to be a positive response to atrial stretch due to the electrical stimulation. Therefore, we conclude that PU-GNT/NW scaffolds can accelerate cardiomyocyte response to the stresses induced by electrical stimulation, decreasing the progress of cardiac hypertrophy. NPPB marks any overstretching in myocardial tissue and acts similar to ANF, but with lower affinity. As it has been shown that in native heart, mechanical stretch is initiated by electrical signals [58], increases in the expression levels of these genes reflect the overstretching of the cell-scaffold constructs, particularly in the PU-50 samples (Fig. 4a).

Similarly, incorporation of gold induced in our studies a significant increase in gene expression level of the early cardiac transcription factors Nkx2.5 and Mef2c (Fig. 4c). Mef2c play a role in myogenesis, maintaining the differentiated state of muscle cells. Nkx2.5 also functions in heart formation and development [5, 15]. This implies that 50 ppm of GNT/NW is an optimum concentration for stimulating the expression levels of important cardiac differentiation markers and of myogenesis.

## 5. Conclusions

In this study we investigated different properties of cardiomyocytes on porous nanocomposite scaffolds formed by a biodegradable polyurethane matrix with incorporated gold nanoparticles (PU-GNT/NW). Cardiomyocyte adhesion and proliferation were strongly increased in response to electrical stimulation on PU-GNT/NW composites within 4 days. After 4 days of incubation and electrical stimulation on the scaffolds, cardiomyocytes on PU-GNT/NW samples showed a more native morphology and enhanced proliferation compared to gold-free PU-0. Only small differences in cell behavior were observed between PU-50 and PU-100, where particularly PU-50 induced optimum cell distribution and spreading, as well as the largest up-regulated expression levels of genes relevant to cardiac differentiation and hypertrophy. Taken together, our data suggest that nanocomposites made from porous and biodegradable polyurethane scaffolds with an optimized content (50 ppm) of gold nanowires/nanotubes in combination with electrical stimulation are promising materials for future applications in cardiac tissue engineering.

## Acknowledgements

We would like to thank Manuela Lieb for her advice, guidance and assistance during the cell study. Furthermore we would like to thank Hilke Clasen (Institute of Immunology) for skillful technical assistance with RNA-isolation, cDNA synthesis and (q)PCR. The Boehringer Ingelheim Fonds is also acknowledged for supporting Y. Ganji's stay at the University of Kiel by a travel grant. Furthermore, Q. L. and C. S. acknowledge funding from the Deutsche Forschungsgemeinschaft (DFG) through the SFB 677 (project B11) and grant SE 1801/2-1, as well as from the European Research Council (ERC Starting Grant no. 336104). We thank Brook Shurtleff for proofreading the manuscript.

## References:

[1] Lloyd-Jones D, Adams RJ, Brown TM, Carnethon M, Dai S, De Simone G, et al. Heart disease and stroke statistics—2010 update. Circulation 2010;121:e46-e215.

[2] Teerlink JR, Cotter G, Davison BA, Felker GM, Filippatos G, Greenberg BH, et al. Serelaxin, recombinant human relaxin-2, for treatment of acute heart failure (RELAX-AHF): a randomised, placebo-controlled trial. The Lancet 2013;381:29-39.

[3] Terracciano C, Hardy J, Birks E, Khaghani A, Banner N, Yacoub M. Clinical recovery from end-stage heart failure using left-ventricular assist device and pharmacological therapy correlates with increased sarcoplasmic reticulum calcium content but not with regression of cellular hypertrophy. Circulation 2004;109:2263-5.

[4] Bar A, Haverich A, Hilfiker A. Cardiac tissue engineering:" reconstructing the motor of life". Scandinavian journal of surgery 2007;96:154.

[5] Guan J, Wang F, Li Z, Chen J, Guo X, Liao J, et al. The stimulation of the cardiac differentiation of mesenchymal stem cells in tissue constructs that mimic myocardium structure and biomechanics. Biomaterials 2011;32:5568-80.

[6] Stamm C, Westphal B, Kleine HD, Petzsch M, Kittner C, Klinge H, et al. Autologous bone-marrow stem-cell transplantation for myocardial regeneration. The Lancet 2003;361:45-6.

[7] Turner WS, Wang X, Johnson S, Medberry C, Mendez J, Badylak SF, et al. Cardiac tissue development for delivery of embryonic stem cell‐derived endothelial and cardiac cells in natural matrices. Journal of Biomedical Materials Research Part B: Applied Biomaterials 2012;100:2060-72.

[8] Li Z, Guan J. Hydrogels for cardiac tissue engineering. Polymers 2011;3:740-61.

[9] Giraud M-N, Armbruster C, Carrel T, Tevaearai HT. Current state of the art in myocardial tissue engineering. Tissue Engineering 2007;13:1825-36.

[10] Zhao Z, Qin L, Reid B, Pu J, Hara T, Zhao M. Directing Migration of Endothelial Progenitor Cells with Applied DC Electric Fields. Stem Cell Research 2012;8:38-48.

[11] Kasper G, Dankert N, Tuischer J, Hoeft M, Gaber T, Glaeser J, et al. Mesenchymal stem cells regulate angiogenesis according to their mechanical environment. Stem Cells 2007;25:903-10.
[12] Bai H, Forrester JV, Zhao M. DC electric stimulation upregulates angiogenic factors in endothelial cells through activation of VEGF receptors. Cytokine 2011.
[13] Singelyn JM, DeQuach JA, Seif-Naraghi SB, Littlefield RB, Schup-Magoffin PJ, Christman KL. Naturally derived myocardial matrix as an injectable scaffold for cardiac tissue engineering. Biomaterials 2009;30:5409-16.
[14] Gaballa MA, Sunkomat JNE, Thai H, Morkin E, Ewy G, Goldman S. Grafting an acellular 3-dimensional collagen scaffold onto a non-transmural infarcted myocardium induces neo-angiogenesis and reduces cardiac remodeling. The Journal of heart and lung transplantation 2006;25:946-54.
[15] Gaetani R, Doevendans PA, Metz CHG, Alblas J, Messina E, Giacomello A, et al. Cardiac tissue engineering using tissue printing technology and human cardiac progenitor cells. Biomaterials 2012;33:1782e90.
[16] Christman KL, Vardanian AJ, Fang Q, Sievers RE, Fok HH, Lee RJ. Injectable fibrin scaffold improves cell transplant survival, reduces infarct expansion, and induces neovasculature formation in ischemic myocardium. Journal of the American College of Cardiology 2004;44:654-60.
[17] Stout DA, Basu B, Webster TJ. Poly (lactic–co-glycolic acid): Carbon nanofiber composites for myocardial tissue engineering applications. Acta Biomaterialia 2011;7:3101-12.
[18] Park H, Radisic M, Lim JO, Chang BH, Vunjak-Novakovic G. A novel composite scaffold for cardiac tissue engineering. In Vitro Cellular & Developmental Biology-Animal 2005;41:188-96.
[19] Alperin C, Zandstra P, Woodhouse K. Polyurethane films seeded with embryonic stem cell-derived cardiomyocytes for use in cardiac tissue engineering applications. Biomaterials 2005;26:7377-86.
[20] P Prabhakaran M, Kai D, Ghasemi-Mobarakeh L, Ramakrishna S. Electrospun biocomposite nanofibrous patch for cardiac tissue engineering. Biomedical Materials 2011;6:055001.
[21] Da Silva GR. Biodegradation of polyurethanes and nanocomposites to non-cytotoxic degradation products. Polymer degradation and stability 2010;95:491-9.
[22] Guelcher SA, Srinivasan A, Dumas JE, Didier JE, McBride S, Hollinger JO. Synthesis, mechanical properties, biocompatibility, and biodegradation of polyurethane networks from lysine polyisocyanates. Biomaterials 2008;29:1762-75.
[23] Chen Q-Z, Bismarck A, Hansen U, Junaid S, Tran MQ, Harding SE, et al. Characterisation of a soft elastomer poly (glycerol sebacate) designed to match the mechanical properties of myocardial tissue. Biomaterials 2008;29:47-57.
[24] Fujimoto KL, Tobita K, Merryman WD, Guan J, Momoi N, Stolz DB, et al. An elastic, biodegradable cardiac patch induces contractile smooth muscle and improves cardiac remodeling and function in subacute myocardial infarction. Journal of the American College of Cardiology 2007;49:2292-300.
[25] Ayo M, Madufor I, Ekebafe L, Chukwu M, Tenebe O, Eguare K. Performance Analysis of Castor Oil Based Polyurethane Foam. International Journal of Basic and Applied Sciences 2012;1:255-7.
[26] Corcuera M, Rueda L, Fernandez d'Arlas B, Arbelaiz A, Marieta C, Mondragon I, et al. Microstructure and properties of polyurethanes derived from castor oil. Polymer degradation and stability 2010;95:2175-84.
[27] Teramoto N, Saitoh Y, Takahashi A, Shibata M. Biodegradable polyurethane elastomers prepared from isocyanate‐terminated poly (ethylene adipate), castor oil, and glycerol. Journal of applied polymer science 2010;115:3199-204.
[28] Amanpour S, Solouk A, Mirzadeh H, Mohagheghi MA, Rabbani S, Tirgari F. In vitro and in vivo assays of cartilage repair by perforated polyurethane scaffold. Iranian Polymer Journal 2010;19:403-15.
[29] de Oliveira Frazilio F, de Rossi R, Neto JMN, FaccoI GG, Ovando TM, Fialho MPF. Use of castor oil polyurethane in an alternative technique for medial patella surgical correction in dogs. Acta Cirurgica Brasileira 2006;21.

[30] Gorna K, Gogolewski S. Biodegradable porous polyurethane scaffolds for tissue repair and regeneration. Journal of Biomedical Materials Research Part A 2006;79:128-38.
[31] Hou Q, Grijpma DW, Feijen J. Porous polymeric structures for tissue engineering prepared by a coagulation, compression moulding and salt leaching technique. Biomaterials 2003;24:1937-47.
[32] Yoon JJ, Kim JH, Park TG. Dexamethasone-releasing biodegradable polymer scaffolds fabricated by a gas-foaming/salt-leaching method. Biomaterials 2003;24:2323-9.
[33] Kim TG, Chung HJ, Park TG. Macroporous and nanofibrous hyaluronic acid/collagen hybrid scaffold fabricated by concurrent electrospinning and deposition/leaching of salt particles. Acta Biomaterialia 2008;4:1611-9.
[34] Cheung HK, Han TTY, Marecak DM, Watkins JF, Amsden BG, Flynn LE. Composite hydrogel scaffolds incorporating decellularized adipose tissue for soft tissue engineering with adipose-derived stem cells. Biomaterials 2014;35:1914-23.
[35] Tateishi T, Chen G, Ushida T. Biodegradable porous scaffolds for tissue engineering. Journal of Artificial Organs 2002;5:77-83.
[36] Laschke M, Strohe A, Scheuer C, Eglin D, Verrier S, Alini M, et al. In vivo biocompatibility and vascularization of biodegradable porous polyurethane scaffolds for tissue engineering. Acta Biomaterialia 2009;5:1991-2001.
[37] Raic A, Rödling L, Kalbacher H, Lee-Thedieck C. Biomimetic macroporous PEG hydrogels as 3D scaffolds for the multiplication of human hematopoietic stem and progenitor cells. Biomaterials 2014;35:929-40.
[38] Ganji Y, Kasra M, Salahshour Kordestani S, Bagheri Hariri M. Synthesis and Characterization of Gold Nanotube/Nanowire-Polyurethane Composite Based on Castor Oil and Polyethylene Glycol. Materials Science and Engineering: C 2014.
[39] Parrag IC, Zandstra PW, Woodhouse KA. Fiber alignment and coculture with fibroblasts improves the differentiated phenotype of murine embryonic stem cell-derived cardiomyocytes for cardiac tissue engineering. Biotechnology and bioengineering 2012;109:813-22.
[40] Rockwood DN, Akins Jr RE, Parrag IC, Woodhouse KA, Rabolt JF. Culture on electrospun polyurethane scaffolds decreases atrial natriuretic peptide expression by cardiomyocytes in vitro. Biomaterials 2008;29:4783-91.
[41] Li SH, De Wijn JR, Layrolle P, De Groot K. Synthesis of macroporous hydroxyapatite scaffolds for bone tissue engineering. Journal of biomedical materials research 2002;61:109-20.
[42] Rasband W. 2009. ImageJ, US National Institutes of Health, Bethesda, Maryland, USA. 1997.
[43] Serena E, Figallo E, Tandon N, Cannizzaro C, Gerecht S, Elvassore N, et al. Electrical stimulation of human embryonic stem cells: cardiac differentiation and the generation of reactive oxygen species. Experimental cell research 2009;315:3611-9.
[44] Tandon N, Cannizzaro C, Chao PHG, Maidhof R, Marsano A, Au HTH, et al. Electrical stimulation systems for cardiac tissue engineering. Nature protocols 2009;4:155-73.
[45] Ounzain S, Kobayashi S, Peterson RE, He A, Motterle A, Samani NJ, et al. Cardiac expression of ms1/STARS, a novel gene involved in cardiac development and disease, is regulated by GATA4. Molecular and cellular biology 2012;32:1830-43.
[46] Hu X, Li T, Zhang C, Liu Y, Xu M, Wang W, et al. GATA4 regulates ANF expression synergistically with Sp1 in a cardiac hypertrophy model. Journal of cellular and molecular medicine 2011;15:1865-77.
[47] Tan SC, Carr CA, Yeoh KK, Schofield CJ, Davies KE, Clarke K. Identification of valid housekeeping genes for quantitative RT-PCR analysis of cardiosphere-derived cells preconditioned under hypoxia or with prolyl-4-hydroxylase inhibitors. Molecular biology reports 2012;39:4857-67.
[48] Bangaru MLY, Park F, Hudmon A, McCallum JB, Hogan QH. Quantification of gene expression after painful nerve injury: validation of optimal reference genes. Journal of Molecular Neuroscience 2012;46:497-504.

590 [49] Dvir T, Timko BP, Brigham MD, Naik SR, Karajanagi SS, Levy O, et al. Nanowired three-dimensional
591 cardiac patches. Nature Nanotechnology 2011;6:720-5.
592 [50] Drury JL, Dennis RG, Mooney DJ. The tensile properties of alginate hydrogels. Biomaterials
593 2004;25:3187-99.
594 [51] Hsu S-h, Tang C-M, Tseng H-J. Biostability and biocompatibility of poly (ester urethane)–gold
595 nanocomposites. Acta Biomaterialia 2008;4:1797-808.
596 [52] McBane JE, Cai K, Labow RS, Paul Santerre J. Co-culturing monocytes with smooth muscle cells
597 improves cell distribution within a degradable polyurethane scaffold and reduces inflammatory
598 cytokines. Acta Biomaterialia 2012;8:488-501.
599 [53] Santerre J, Woodhouse K, Laroche G, Labow R. Understanding the biodegradation of polyurethanes:
600 from classical implants to tissue engineering materials. Biomaterials 2005;26:7457-70.
601 [54] Alkilany AM, Murphy CJ. Toxicity and cellular uptake of gold nanoparticles: what we have learned so
602 far? Journal of nanoparticle research 2010;12:2313-33.
603 [55] Hsu S, Tang CM, Tseng HJ. Gold nanoparticles induce surface morphological transformation in
604 polyurethane and affect the cellular response. Biomacromolecules 2008;9:241-8.
605 [56] Vunjak-Novakovic G, Tandon N, Godier A, Maidhof R, Marsano A, Martens TP, et al. Challenges in
606 cardiac tissue engineering. Tissue Engineering Part B: Reviews 2010;16:169-87.
607 [57] Kennedy JP, McCandless SP, Lasher RA, Hitchcock RW. The mechanically enhanced phase separation
608 of sprayed polyurethane scaffolds and their effect on the alignment of fibroblasts. Biomaterials
609 2010;31:1126-32.
610 [58] Radisic M, Park H, Gerecht S, Cannizzaro C, Langer R, Vunjak-Novakovic G. Biomimetic approach to
611 cardiac tissue engineering. Philosophical Transactions of the Royal Society B: Biological Sciences
612 2007;362:1357-68.
613 [59] Au HTH, Cheng I, Chowdhury MF, Radisic M. Interactive effects of surface topography and pulsatile
614 electrical field stimulation on orientation and elongation of fibroblasts and cardiomyocytes. Biomaterials
615 2007;28:4277-93.
616 [60] Makino S, Fukuda K, Miyoshi S, Konishi F, Kodama H, Pan J, et al. Cardiomyocytes can be generated
617 from marrow stromal cells in vitro. Journal of Clinical Investigation 1999;103:697.
618 [61] Temsah R, Nemer M. GATA factors and transcriptional regulation of cardiac natriuretic peptide
619 genes. Regulatory peptides 2005;128:177-85.
620